Microfluidic Assembly of a Multifunctional Tailorable Composite System Designed for Site Specific Combined Oral Delivery of Peptide Drugs

Francisca Araújo,[∥,†,‡,§] Neha Shrestha,[∥] Mohammad-Ali Shahbazi,[∥] Dongfei Liu,[∥] Bárbara Herranz-Blanco,[∥] Ermei M. Mäkilä,[∥,⊥] Jarno J. Salonen,[⊥] Jouni T. Hirvonen,[∥] Pedro L. Granja,[†,‡,§] Bruno Sarmento,*[,†,‡,#] and Hélder A. Santos*[,∥]

[∥]Division of Pharmaceutical Chemistry and Technology, Faculty of Pharmacy, University of Helsinki, FI-00014 Helsinki, Finland, [†]Instituto de Investigação e Inovação em Saúde, Universidade do Porto, 4150-180 Porto, Portugal, [‡]INEB — Instituto de Engenharia Biomédica, University of Porto, 4150-180 Porto, Portugal, [§]ICBAS — Instituto Ciências Biomédicas Abel Salazar, University of Porto, 4150-180 Porto, Portugal, [⊥]Laboratory of Industrial Physics, University of Turku, FI-20014 Turku, Finland, and [#]CESPU, Instituto de Investigação e Formação Avançada em Ciências e Tecnologias da Saúde, 4585-116 Gandra, Portugal

ABSTRACT Multifunctional tailorable composite systems, specifically designed for oral dual-delivery of a peptide (glucagon-like peptide-1) and an enzymatic inhibitor (dipeptidyl peptidase 4 (DPP4)), were assembled through the microfluidics technique. Both drugs were coloaded into these systems for a synergistic therapeutic effect. The systems were composed of chitosan and cell-penetrating peptide modified poly(lactide-*co*-glycolide) and porous silicon nanoparticles as nanomatrices, further encapsulated in an enteric hydroxypropylmethylcellulose acetylsuccinate polymer. The developed multifunctional systems were pH-sensitive, inherited by the enteric polymer, enabling the release of the nanoparticles only in the simulated intestinal conditions. Moreover, the encapsulation into this polymer prevented the degradation of the nanoparticles' modifications. These nanoparticles showed strong and higher interactions with the intestinal cells in comparison with the nonmodified ones. The presence of DPP4 inhibitor enhanced the peptide permeability across intestinal cell monolayers. Overall, this is a promising platform for simultaneously delivering two drugs from a single formulation. Through this approach peptides are expected to increase their bioavailability and efficiency *in vivo* both by their specific release at the intestinal level and also by the reduced enzymatic activity. The use of this platform, specifically in combination of the two antidiabetic drugs, has clinical potential for the therapy of type 2 diabetes mellitus.

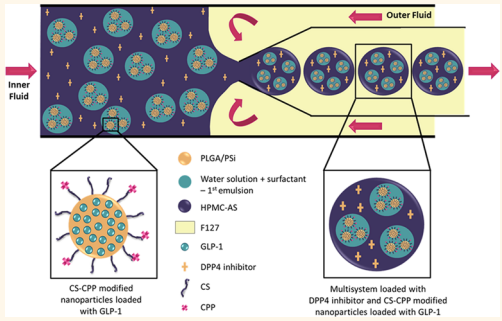

KEYWORDS: chitosan · dual-delivery · microfluidics · PLGA · porous silicon

Nanoparticles composed of biocompatible and biodegradable materials have been claimed as promising candidates toward the oral administration of peptides.[1,2] These nanoparticles enhance the oral bioavailability of peptides and control their release, as well as provide a preserved environment for the encapsulated drugs.[3−5]

Among the mostly studied materials, poly(lactic-*co*-glycolic acid) (PLGA) and mesoporous silicon (PSi) have attracted a lot of attention, becoming the most desirable materials in the drug delivery field for the administration of macromolecules.[6,7] In one hand, PLGA features can be modulated by the ratio between the monomers that constitute the polymer, exhibiting a wide range of erosion times, favorable degradation characteristics and tunable mechanical properties. It can be used to encapsulate numerous drugs with different physicochemical properties and also to sustain their release.[8,9] Moreover, it has extensive clinical applications, being already approved by the Food and Drug Administration (FDA) and the European Medicine Agency (EMA) for parenteral administration.[9] On the other

* Address correspondence to bruno.sarmento@ineb.up.pt, helder.santos@helsinki.fi.

Received for review May 7, 2015 and accepted August 2, 2015.

Published online August 02, 2015
10.1021/acsnano.5b02762

hand, PSi nanoparticles have large surface area, pore volumes with adjustable diameters (2−50 nm), as well as higher drug loading capacity compared to the majority of the other materials.[10−12] Furthermore, the drug loading is usually a simple process where the drug is retained inside the mesopores by physical adsorption or electrostatic interactions.[10] Nevertheless, the oral delivery of PLGA and PSi nanoparticles is not in such advanced state. The negative surface charge of the nanoparticles tends to limit their interaction with the negatively charged cell's surface, which is further intensified by the rapid turnover of the mucus and the intestinal cells.[4]

To tackle the limitations of these oral drug nanocarriers, the nanoparticles can be tailored with other materials to yield a variety of physical properties to overcome the main intestinal barriers, such as the mucus layer, epithelium and enzymatic degradation.[13,14] Chitosan (CS) and cell penetrating peptides (CPPs) are polycationic molecules extensively used in the drug delivery field. CS is a biopolymer that has been mainly used to modify nanoparticles due to its mucoadhesive characteristics and its properties as an intestinal permeability enhancer by transiently open the tight junctions existing between the epithelial cells.[15−17] CPPs were originally considered as a "Trojan horse" because of their ability to enter cells without causing damage or eliciting a cellular response,[18,19] increasing the transcellular transport.[20] Yet, a major challenge still remains for the oral delivery of peptides in order to overcome the harsh conditions of the stomach. In this regard, pH-sensitive polymers have been frequently employed in the drug formulation and/or coating of nano- and microparticles to protect them from the very acidic gastric pH.[11,21]

In this study, we developed novel multifunctional systems that can simultaneously load peptides and enzymatic inhibitors in a single carrier with the aim to resist the conditions of the stomach, to enhance the nanoparticle's interactions with the intestinal mucus and epithelium, and to protect the peptides from enzymatic degradation after the release. An antidiabetic peptide, glucagon-like peptide-1 (GLP-1), is in the pipeline for the type 2 diabetes mellitus (T2DM) therapy, and was used here as a model peptide. Because of its poor intestinal permeability, GLP-1 needs to be administrated by parenteral route, resulting in poor patient compliance.[22,23] Moreover, the success of the GLP-1 therapy is hindered by its rapid degradation (<2 min) by the dipeptidyl peptidase 4 (DPP4) enzyme produced in the intestine.[24] Therefore, in order to achieve an efficient release and permeability across the intestinal epithelium of active GLP-1, the antidiabetic peptide was loaded into different nanoparticles composed of PLGA and PSi biomaterials. The PLGA and PSi nanoparticles were further modified with the mucoadhesive polymer CS and with an oligoarginine CPP to increase the permeability of nanoparticles across the intestinal cells. Afterward, the nanoparticulate systems were encapsulated within an enteric polymer hydroxypropylmethylcellulose acetylsuccinate (HPMC-AS) loaded with the DPP4 inhibitor, using the microfluidics technique (Scheme 1). To the best of our knowledge,

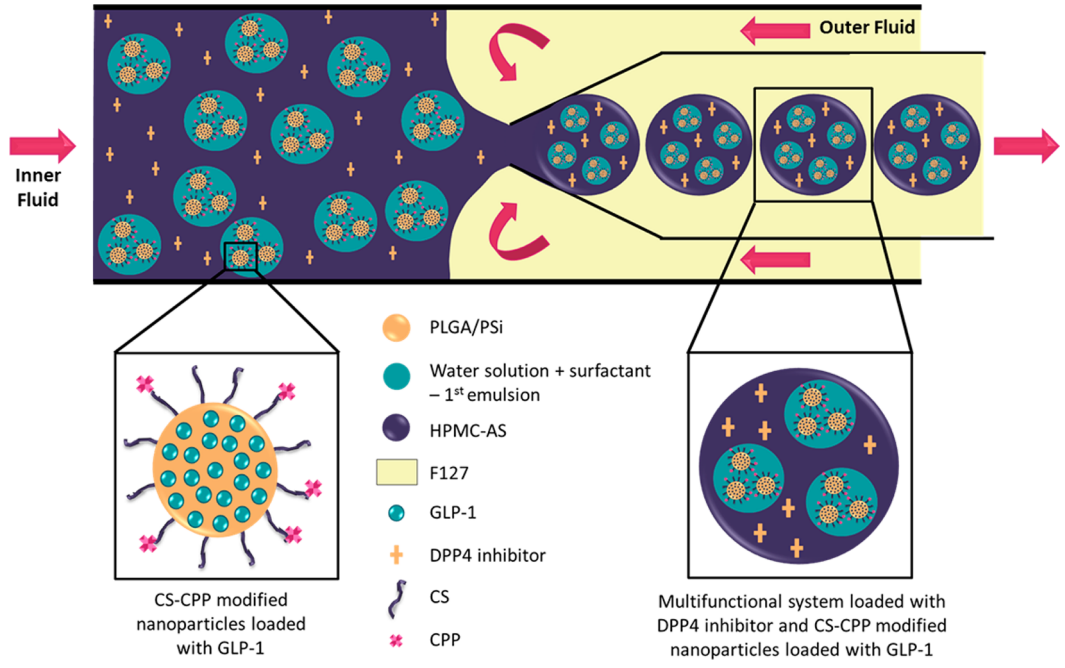

Scheme 1. Schematic representation of the microfluidics approach used to produce the pH-responsive systems, coloaded with GLP-1 and DPP4 inhibitor. The inner fluid consisted of modified PLGA and PSi nanoparticles and the enteric polymer dissolved in ethyl acetate. The antidiabetic peptide GLP-1 was loaded into the modified nanoparticles, whereas the enzymatic DPP4 inhibitor was dissolved directly in the inner fluid. The outer continuous fluid was an aqueous solution of F127 (2% w/v), which could efficiently stabilize the oil/water (O/W) interface.

this is the first time that the combination of these two drugs was formulated in a single delivery system. This innovative approach produced monodisperse and uniform particulate structures with the desired composition.[11,21] In comparison to the conventional preparation methods with microfluidics, by tuning the flow rates of the immiscible fluids, emulsions are formed with an exquisite degree of control and rather high encapsulation efficiency.[25,26] The resultant multifunctional systems were then characterized for size, morphology, pH-responsiveness, drug release, and synergistic antidiabetic peptide GLP-1 permeability across a triple intestinal cell coculture model[27] in the presence of the enzymatic DPP4 inhibitor. The inhibition capacity of the DPP4 enzyme activity was also evaluated.

RESULTS AND DISCUSSION

Characterization of the Multifunctional Systems. After the production of the nanoparticles and the CS−CPP surface functionalization, the nanoparticles were characterized in respect to mean size, polydispersity index (PdI), surface charge, association efficiency (AE) and loading degree (LD), as shown in Table 1. Both the unmodified PLGA and PSi nanoparticles presented a *Z*-average size of *ca.* 200 nm with a PdI below 0.1, and negative surface charges. In order to increase the interaction of the nanoparticles with the negatively charged intestinal mucus layer and to improve the permeability of the antidiabetic peptide GLP-1 across the intestinal cells, the nanoparticles were coated first with CS to form PLGA+CS and PSi+CS nanoparticles.[7,8,28] The CS-modified nanoparticles showed an increase in their size and conversion of the zeta-potentials to positive values, demonstrating the successful CS coating of the nanoparticles.[7,8,13,28] In order to improve the transcellular transport, the CS-coated nanoparticles were further modified by covalent attachment of polyarginine R9 CPP to the amine groups of the CS. CPPs, such as R9, are small peptides of few acidic amino acid residues with a high positive charge.[20] Such CPPs are known to have a positive role in the translocation of some drugs across the intestinal epithelium, increasing their oral bioavailability.[29−33] Overall, when modified with CS and CPP (to form PLGA+CS-CPP and PSi+CS-CPP particles), the nanoparticles presented higher particle sizes than the unmodified ones, without significant change in the zeta-potential values (Table 1). Together with the size and charge, the similarity in the AE and LD values indicated the high homogeneity of the nanoparticles from batch-to-batch.[7]

The CS-CPP modified nanoparticles were further encapsulated within an enteric polymer, HPMC-AS, through the microfluidics technique, for their protection, as well as for the protection of the CS and CPP, at the low pH conditions of the gastric environment, originating the H-PLGA+CS-CPP and H-PSi+CS-CPP particles. The microfluidics technique has brought revolutionary impact in the pharmaceutical technology field by manipulating nanoliter volumes, in microscale fluidic channels, with high precision and reduced consumption of reagents.[34,35] In contrast with the conventional production methods, which yield a polydisperse population with drug loading levels less than ideal, with the microfluidics technique the efficiency of encapsulation is near 100%, the particles formed are stable, homogeneous and can be size-controlled.[11,21] Moreover, it can be applicable for diverse constituent fluids, with various chemical compositions and to different cargos, making it a promising technique for the production of several drug delivery systems.[36] The flow-focusing geometry used in this work is a droplet-based method widely used to produce different types of fluid entities on a continuous basis by applying an extensional coflow.[36] In this method, fluids are forced through a narrow orifice where high shear and capillary instability break bubbles off the tip, forming monodisperse emulsion droplets.[21]

As shown by the scanning electron microscopy (SEM) (Figure 1), the produced particles (control group, pH 4.0) had a regular and spherical shape with smooth surface and size around 59.44 ± 8.01 μm. The SEM images also showed a homogeneous size distribution, suggesting the production of monodisperse particles by the microfluidic technique.[11] The DPP4 inhibitor encapsulation efficiency was 20 ± 5%. Considering the amount (mass) of DPP4 inhibitor in the final formulation and that the IC_{50} of the DPP4 inhibitor is of 14 nM, the amount of inhibitor present in the current formulation should be more than enough to be active and to inhibit the enzyme activity efficiently. However, higher

TABLE 1. Characterization of the Nanoparticles in Respect to Their Size, PdI, Zeta-Potential (ζ-Potential), AE and LD of GLP-1 of Different Nanoparticles[a]

sample	size (nm)	PdI	ζ-potential (mV)	AE (%)	LD (%)
PLGA	199.0 ± 4.1	0.08 ± 0.02	−23.6 ± 0.2	58.9 ± 6.9	0.14 ± 0.03
PLGA+CS	243.0 ± 2.2	0.26 ± 0.01	24.8 ± 2.7	59.7 ± 0.7	0.07 ± 0.01
PLGA+CS-CPP	277.2 ± 3.8	0.32 ± 0.02	21.6 ± 3.8	59.7 ± 0.7	0.07 ± 0.01
PSi	193.7 ± 3.0	0.09 ± 0.03	−16.3 ± 0.3	75.0 ± 0.6	15.00 ± 0.05
PSi+CS	282.9 ± 8.0	0.34 ± 0.02	19.2 ± 0.4	75.0 ± 0.5	7.50 ± 0.03
PSi+CS-CPP	320.0 ± 9.8	0.33 ± 0.02	19.1 ± 1.0	75.0 ± 0.5	7.50 ± 0.03

[a] Results are presented as mean ± standard deviation, $n \geq 3$.

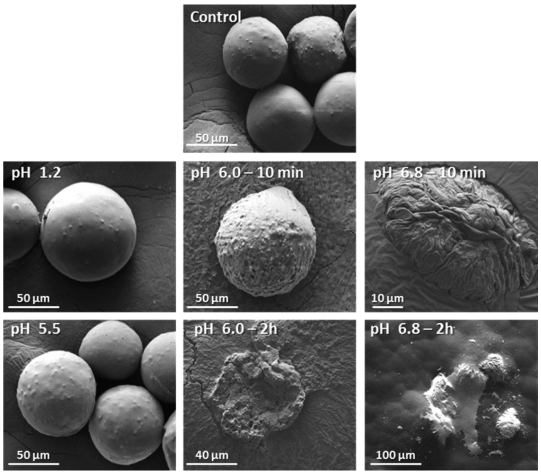

Figure 1. Dissolution behavior of the CS-CPP modified nanoparticles encapsulated in the HPMC-AS polymer at different pH conditions of 1.2 and 5.5 for 2 h, and at pH 6.0 and 6.8 for 10 min and 2 h. The SEM images show the morphology of the prepared particles. The control group was composed by particles at pH 4.0. At pH values below 6.0 the structural integrity of the particles was maintained. At pH 6.0 and 6.8 the structure of the polymeric matrix was destroyed by the dissolution of the polymer.

values can certainly be obtained in the final formulation, for example, by increasing the viscosity of the system (*e.g.*, the viscosity of the HPMC-AS polymer) in order to retain strongly the DPP4 inhibitor in the polymer matrix, by increasing the osmolality of the collection solution or the solution viscosity, or by encapsulating the DPP4 in the nanoparticles either together with the GLP-1 or alone.

pH-Sensitive Response of the Multifunctional Systems. HPMC-AS is a polymer insoluble in acidic conditions and highly soluble at neutral or alkaline pH (pH > 6.0).[11] To evaluate whether the prepared nanoparticles were successfully encapsulated in the polymer and whether the multifunctional system could stand the harsh conditions of the stomach, the particles were observed under SEM at different pH conditions. As shown in Figure 1, at pH 1.2 and 5.5, the shape and surface morphology of particles were regular and smooth, similarly to the observed control particles, showing that the HPMC-AS encapsulation using the microfluidics technique was effective and that the nanoparticles were protected at the acidic conditions. When the multifunctional particulate system was in contact with buffer at pH 6.0, the polymer started to dissolve and the particles' structure started to be compromised already after the first 10 min. After 2 h of incubation, the surface of the particles appeared rough with some visible holes as an indication for the dissolution of the polymer. At pH 6.8, this behavior was even more pronounced with greater changes in the particles' structure during the first 10 min. After 2 h the polymer was completely dissolved. These results are in accordance with the pH responsive characteristics of the polymer, as described elsewhere.[11,21]

Cell Viability Studies. The viability studies were performed in three different cell lines at two different time points and using different concentrations of the particles. AGS is a gastric epithelial cell line originated from human gastric adenocarcinoma,[37] and the cell viability was assessed after 3 h of incubation with the particulate systems. Caco-2 and HT29-MTX are intestinal cell lines originated from colon adenocarcinomas, representing the enterocytes and mucus producing goblet cells,[27,38] respectively, and their viability was measured after 12 h of incubation with the particles. Testing these three cell lines in the two different time points covered the maximum transit time that the particles would be in the stomach and intestine when orally administered, making this a suitable assay to understand whether there is any concentration or component dependent toxicity.[7,39] Nonmodified nanoparticles, CS-CPP-modified nanoparticles, and CS-CPP modified nanoparticles further encapsulated with HPMC-AS particles were tested.

With regards to the PLGA systems, it was observed in the three cell lines studied, that none of the nonmodified nanoparticles, CS-CPP modified nanoparticles and CS-CPP modified nanoparticles encapsulated with HPMC-AS presented toxicity at the tested concentrations, as depicted in Figure 2. PLGA is commonly accepted for its low cytotoxic and good biocompatibility and biodegradability properties, and has already been approved by the FDA for clinical use.[18,29] On the other hand, positively charged particles are usually described as interacting more with the surface of the cell membranes than the negatively charged particles, which may lead to higher cellular cytotoxicity.[40,41] However, in this study, despite the positive surface charge of the CS-CPP modified nanoparticles, no decrease in cell viability was observed in all the cell lines tested. This indicates that the amounts of CS and CPP used did not trigger cytotoxicity reaction, and thus, could be considered as safe for oral drug administration purposes. Previously, some studies have also demonstrated that certain CPPs, including oligoarginine, did not cause any harm to the intestinal epithelial cells.[33,42]

HPMC-AS has been used as a pharmaceutical excipient and has a median lethal dose (LD_{50}) higher than 2.5 g kg^{-1}, which is much higher than the amounts used in our particle formulation.[43] Moreover, the organic solvent used to dissolve the polymer, ethyl acetate (EA), is considered a rather nontoxic organic solvent,[44] and it is believed that no residues of the solvent would be present in the final formulation. In fact, due to its high solubility in water, EA presented a fast diffusion rate to this solvent, which allowed the fast solidification of the particles in the collecting solution, after their formation in the microfluidics device.[21,44]

For the PSi particles, it was observed that the nonmodified nanoparticles, CS-CPP modified nanoparticles, and the CS-CPP modified nanoparticles encapsulated

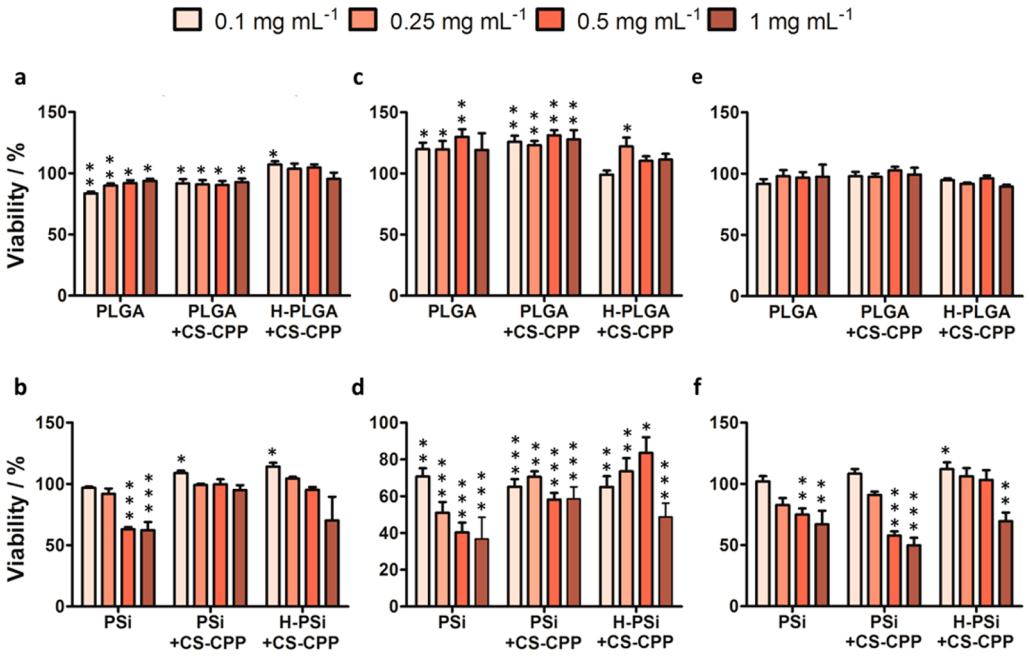

Figure 2. Cell viability levels of the gastric and intestinal cells after exposure to the particles assessed by the CellTiter-Glo luminescence assay. Viability of AGS after 3 h of incubation with different particles concentrations at 37 °C (a and b). Viability of Caco-2 (c and d), and HT29-MTX (e and f) cells after 12 h incubation with different particle concentrations at 37 °C. All the data sets were compared to the negative control (Hank's Balanced Salt Solution, HBSS) using a Student's *t*-test with an unpaired post-test. Error bars represent mean ± standard deviation ($n \geq 3$), and set at probabilities of *$p < 0.05$, **$p < 0.01$, and ***$p < 0.001$.

with HPMC-AS presented concentration dependent cytotoxicity values. The CS-CPP modified nanoparticles presented higher viability values than the nonmodified ones with the exception of the HT29-MTX cells. This behavior may be related to the presence of CS on the surface of the nanoparticles, which would increase the interaction of the nanoparticles with the mucus secreting cells due to the mucoadhesive properties,[39] as described elsewhere.[7] When the pH-sensitive polymer was used to encapsulate the CS-CPP modified nanoparticles, there were no statistically significant changes in the viability of the three cell lines. Although there was a tendency for improved cell viability values by the encapsulated nanoparticles compared to the nonencapsulated ones.

***In Vitro* Release Studies.** To confirm the successful protection of the CS-CPP modified nanoparticles and the loaded drugs from the acidic gastric conditions, as well as to predict the release profiles of the antidiabetic peptide GLP-1 and the enzymatic DPP4 inhibitor, *in vitro* release studies were performed. In order to mimic the environment of the stomach, the study was conducted at pH 1.2 for 2 h. Similarly, to mimic the intestinal environment, the study was performed using simulated fasted state intestinal fluid (FaSSIF) at pH 6.8 for 6 h. The time points chosen are similar to the estimated time for the gastric and intestinal transit, respectively.[7]

The release profiles of GLP-1 from the H-PLGA+CS-CPP and H-PSi+CS-CPP particles at pH 1.2 and 6.8 are shown in Figure 3a and 3b, respectively. At pH 1.2, during the 2 h, the release of GLP-1 was less than 2% and 5% from the PLGA and PSi systems, respectively. However, at pH 6.8 the amount of GLP-1 released from particles was higher, reaching 40% release after 6 h for both the systems. For the H-PLGA+CS-CPP particles, the release was sustained along with the time, unlike in the case of H-PSi+CS-CPP release profile, in which there was a GLP-1 burst release, with 40% of the peptide released in the first 30 min and a very slow release thereafter. These biphasic release patterns dependent on the pH-value confirmed the controlled properties of encapsulation with the enteric polymer, and thus confirmed the fact that the CS-CPP modified nanoparticles and GLP-1 were indeed protected from the acidic conditions. These results are also in agreement with previous studies using the enteric polymer for oral drug delivery.[11] The differences observed in the amounts that were released from H-PLGA+CS-CPP and H-PSi+CS-CPP over time were related with the characteristics of each nanoparticle and the methods used to load the GLP-1 in both of them. In PLGA nanoparticles, the GLP-1 was encapsulated inside of a polymer matrix, while in the PSi nanoparticles the GLP-1 was loaded mainly through physical adsorption in the pores of the nanoparticles, which allowed a faster release.[7]

With regards to the enzymatic DPP4 inhibitor the release was not pH dependent, unlike to what was observed for GLP-1. As it can be observed in Figure 3c and 3d, 80% of the DPP4 inhibitor was released at

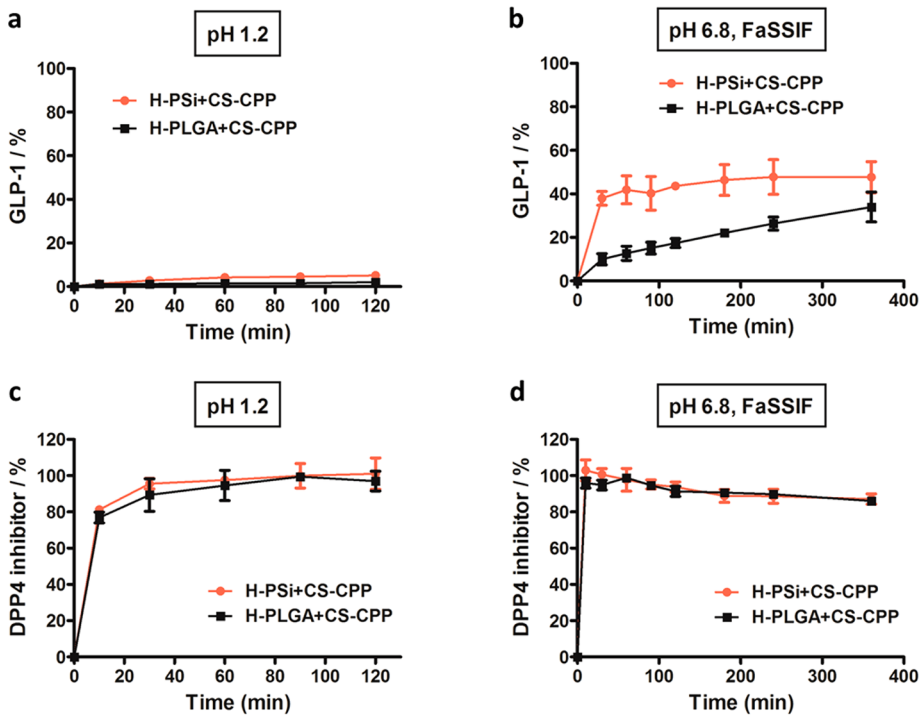

Figure 3. Release profiles of the GLP-1 and the enzymatic DPP4 inhibitor from H-PLGA+CS-CPP and H-PSi+CS-CPP particles at pH 1.2 (a and c) for 2 h and at pH 6.8 (b and d) for 6 h. All the experiments were performed at 37 °C and 100 rpm. The statistical analysis was done using a one-way analysis of variance (ANOVA) with a Bonferroni post-test. Error bars represent the mean ± standard deviation (n = 3).

pH 1.2 during the first 30 min for both the formulations, reaching 100% release in less than 1 h. This can be explained by the very high solubility of the inhibitor in both aqueous solutions and in the organic solvents.[44] The double emulsion technique could retain the aqueous solution in the organic solvent, and thus retain the CS-CPP modified nanoparticles dispersed in water, until the complete polymer dissolution. However, this was not efficient in retaining the enzymatic DPP4 inhibitor and it started to diffuse into the organic solvent. When the particles were collected, the organic solvent started to diffuse to the water due to its high solubility. With the fast solidification process of the microdroplets, the DPP4 inhibitor was trapped in the outer layer of HPMC-AS matrix leading to the release of the enzymatic DPP4 inhibitor.[44] Nevertheless, the enzymatic DPP4 inhibitor has been reported to be successfully administrated orally by adding it into the food and water, without compromising its activity, meaning that the enzymatic DPP4 inhibitor can resist the harsh conditions of the stomach.[45,46]

Cell−Particle Interaction Studies. Once in the small intestine, the CS-CPP modified nanoparticles were completely unconfined due to the dissolution of the pH-sensitive polymer. The interactions of the CS-CPP modified nanoparticles were analyzed qualitatively using confocal fluorescence microscopy and quantitatively by flow cytometry experiments. For the confocal microscopy and flow cytometry experiments, the nanoparticles were labeled with Alexa Fluor 488 hydrazine (green fluorescence emission), as detailed in Supporting Information (SI), and the cell membranes were labeled with CellMask Red (red fluorescence emission). In line with the viability experiments, the Caco-2 and HT29-MTX cells, which are representative of the majority of the intestinal cells, were used to perform the cell−particle interaction studies. A ratio of 90:10 for Caco-2 and HT29-MTX cells, respectively, was used in order to mimic the physiological conditions of the intestine.[27] The confocal fluorescence microscopy results are shown in Figure 4a.

It was observed that for the unmodified nanoparticles there were no significant interactions with the cells for either the PLGA or the PSi nanoparticles. When the nanoparticles were modified with CS, the cell−nanoparticle interactions were greatly increased and many of the nanoparticles were observed in the close vicinity of the cell membranes. This increase in interaction could be due to the cationic nature and the mucoadhesive properties of the CS, causing strong electrostatic interactions with the mucus producing cells of the coculture,[8,47] as described elsewhere.[7,39] After the modifications with CS and CPP, the cell−nanoparticle interactions were even higher as compared to the nonmodified nanoparticles, as more nanoparticles were associated with the cells' surface. In this case, the nanoparticles were interacting with the cell membranes and were also taken up by the cells. Even after the encapsulation with the enteric polymer, and once the polymer was dissolved at a higher pH,

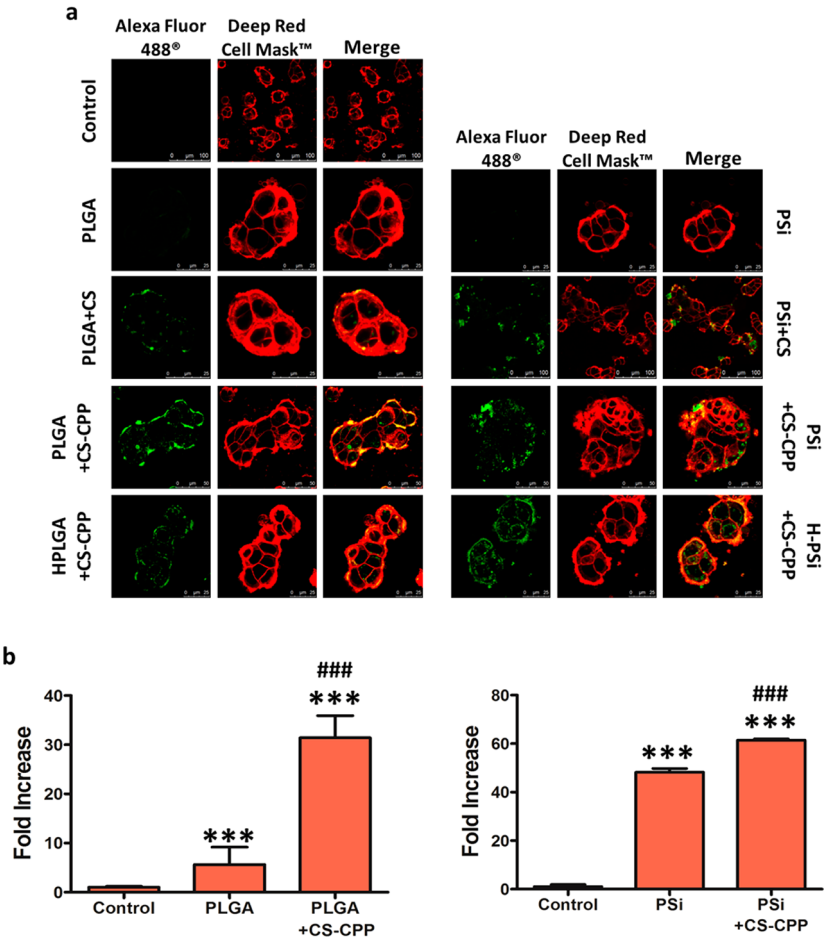

Figure 4. Interactions between the different nanoparticles and the Caco-2/HT29-MTX (90:10) coculture after incubation for 3 h at 37 °C. (a) Confocal microscopy images of the cell membranes stained in red by CellMask Red, and the nanoparticles in green conjugated with Alexa Fluor 488. (b) Flow cytometry quantification of the interactions by PLGA and PSi nanosystems. The results were related to the fold increase of the percentage of cells interacting with the nanoparticles. Data sets were compared to the control (*$p < 0.05$, **$p < 0.01$, and ***$p < 0.001$) and between them ($^{\#}p < 0.05$, $^{\#\#}p < 0.01$, and $^{\#\#\#}p < 0.001$) using a Student's *t*-test with an unpaired post-test. Error bars represent mean ± standard deviation ($n \geq 3$).

the nanoparticles presented a high capacity to interact and to be internalized by the cells. The control groups were just cells in coculture without any particles.

Quantitative studies of the cell−particle interactions with flow cytometry demonstrated that the CS-CPP modified PLGA and CS-CPP modified PSi nanoparticles presented a 5.6-fold and 1.3-fold increase in the interaction with the intestinal cells in the coculture (control group), compared to the unmodified nanoparticles, respectively (Figure 4b). The cationic nature of the CS and the CPP were important features that led to high cell−nanoparticle interactions.[18]

GLP-1 Permeability Across the Intestinal Cell Monolayers in the Presence of DPP4 Inhibitor. The permeability of the antidiabetic peptide GLP-1 was studied for H-PLGA+CS-CPP and H-PSi+CS-CPP particles in the presence and absence of the DPP4 inhibitor. As observed in Figures 5a and S1, the GLP-1 permeation across the monolayers was higher for the H-PSi+CS-CPP particles than for the H-PLGA+CS-CPP particles. The difference between the amounts of GLP-1 that permeated across the cell monolayers by the two systems may be due to the differences observed in the release profiles of GLP-1 loaded in both the particles. For the PSi system, there was observed a burst release of GLP-1 during the first 30 min, while for the PLGA system the release was more sustained over time. Thus, the amount of GLP-1 available to permeate across the cell monolayers in the presence of the PSi system was 2-fold compared to the amount of the PLGA system, which justifies the observed permeability results after 3 h.[7] In the presence of the enzymatic DPP4 inhibitor, the permeability of GLP-1 across the cell monolayers was even higher, with ∼1.5-fold increase for the PSi systems and ∼5-fold increase for the PLGA systems when compared to the permeability values without the enzymatic DPP4 inhibitor (Figure 5b). The synergistic effect of GLP-1 permeation in the presence the enzymatic DPP4 inhibitor is probably due to the inhibition of the DPP4 enzyme, which helped to protect the GLP-1 from degradation when permeating across the cell monolayer. Studies conducted in animal models

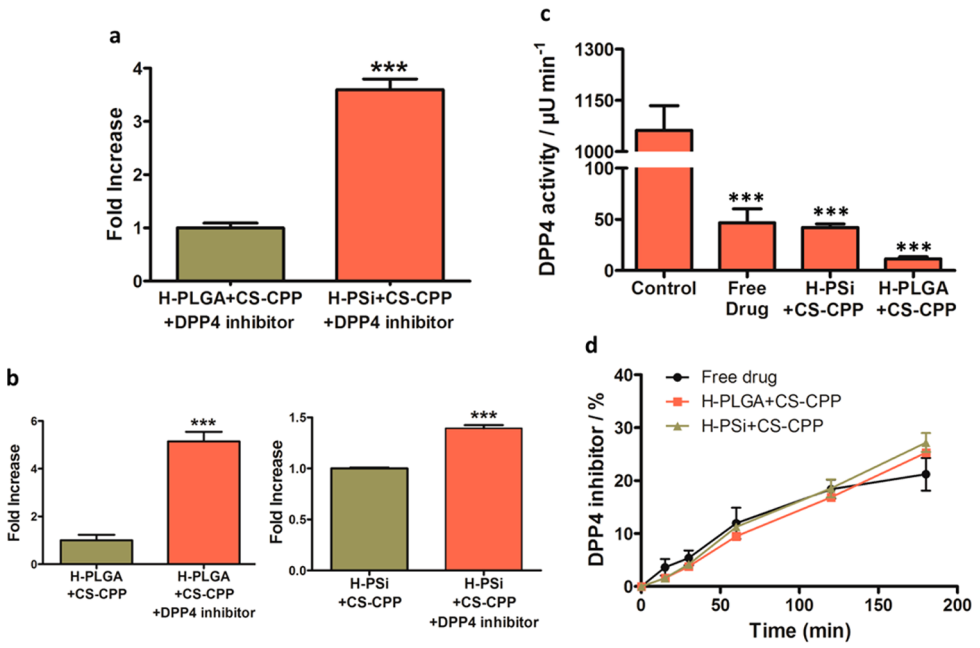

Figure 5. (a) GLP-1 permeability of H-PLGA+CS-CPP and H-PSi+CS-CPP across the Caco-2/HT29-MTX cell monolayers in the presence of DPP4 inhibitor. (b) Differences between GLP-1 permeability across the Caco-2/HT29-MTX cell monolayers in the presence and absence of the DPP4 inhibitor. (c) DPP4 enzymatic activity after cellular incubation with particles loaded with the DPP4 inhibitor. (d) Permeability profiles of DPP4 across the Caco-2/HT29-MTX cell monolayers in the free form and when loaded in both the multifunctional particulate systems. The statistical analysis was done using a Student's *t*-test and one-way analysis of variance (ANOVA) with unpaired and Bonferroni post-test, respectively. Error bars represent mean ± standard deviation ($n \geq 3$), set at probabilities of *$p < 0.05$, **$p < 0.01$, and ***$p < 0.001$.

have shown that when the DPP4 inhibitor was orally administrated, the plasma levels of intact and active GLP-1 were increased, which indicated that it was not rapidly degraded by the DPP4 enzyme.[46,48]

When analyzing the enzymatic activity of DPP4 (Figure 5c) after the 4 h incubation with the particles, it was observed that the enzymatic activity of DPP4 in the cells exposed to the inhibitor was significantly lower for both the PLGA (>20 μU min^{-1}) and PSi systems (40 μU min^{-1}) than in the cells with no exposure to the inhibitor (~1062 μU min^{-1}) (control group). When compared to the free form of the inhibitor, the activity of the inhibitor loaded in the particles was not affected, and despite there being no statistically significant difference, these values were lower than in the case of the free form of DPP4 inhibitor. The similar permeability profiles of the enzymatic DPP4 inhibitor (Figure 5d) across the cell monolayers corroborate these results. It has been shown in *in vivo* studies that in the presence of DPP4 inhibitor the enzymatic activity was changed from 3.26 ± 0.19 mU mL^{-1} to 0.01 ± 0.03 mU mL^{-1}, and that the inhibition of the enzyme was dose dependent.[46,48]

Because DPP4 inhibitor has also been demonstrated as having a positive effect in decreasing the blood glucose levels, it will have an additional benefit to our system for future *in vivo* applications.[46,48−50]

CONCLUSIONS

In this study, two novel multifunctional composite systems were prepared in a highly reproducible, efficient and reliable manner using the innovative microfluidics technique. The systems consisted of CS-CPP modified PLGA and PSi nanoparticles used as nanomatrices encapsulated into an enteric polymer, which were coloaded with an antidiabetic peptide GLP-1 and an enzymatic DPP4 inhibitor. The dual-delivery of these two drugs by the same formulation was for the first time described. Because of the characteristics of the enteric polymer, the multifunctional composite systems were able to protect the CS-CPP modified nanoparticles and consequently prevent the premature release of the peptide and its degradation in the adverse conditions of the gastrointestinal tract. By precisely releasing the CS-CPP modified nanoparticles and subsequently the peptide in the upper intestine, the bioavailability of peptide and its permeation would be greatly improved. Moreover, due to the modifications of the nanoparticles, the interactions and the retention time of the nanoparticles with the intestinal cells were also greatly improved. It was also shown that the release of both the drugs had a synergistic effect since the presence of the enzymatic DPP4 inhibitor decreased drastically the activity of the enzyme, improving further the amount of active peptide permeated across the intestinal cells. Thus, taking particularly into account the GLP-1 peptide and the enzymatic DPP4 inhibitor, these multifunctional particulate systems might be very promising for clinical applications in the therapy of T2DM, due to the potential to increase in GLP-1 half-life in an *in vivo*

situation. Overall, due to the flexibility of the techniques employed here, and the multifunctional character of the particulate systems, they have potential to orally deliver sensitive biomolecules in combination with other drugs with different physicochemical properties.

MATERIALS AND METHODS

Materials and Cell Culture. GLP-1 was purchased from United Peptides (USA). DPP4 inhibitor (NVP DPP 728 dihydrochloride) was purchased from Tocris Bioscience (UK) and CPP R9 was purchased from GenicBio (China). PLGA 50:50 was obtained from Purac Biomaterials, Purasorb PDLG 5004A, The Netherlands. Poly(vinyl alcohol) (PVA), medium molecular weight CS, 2-(*N*-morpholino)-ethanesulfonic acid (MES), 1-ethyl-3-(3-(dimethylamino)-propyl)-carbodiimide (EDC), *N*-hydroxysuccinimide (NHS), 4-(2-hydroxyethyl)-1-piperazineethanesulfonic acid (HEPES) and glutaraldehyde were purchased from Sigma-Aldrich (USA). HPMC-AS was obtained by Shin-Etsu (Japan). Pluronic F127 was purchased from BASF (Germany). Hank's balanced salt solution (HBBS), phosphate buffered saline (PBS), Alexa Fluor 488 hydrazine, Versene and heat inactivated fetal bovine serum (FBS) were purchased from Life Technologies (USA). Dulbecco's Modified Eagle medium (DMEM), Roswell Park Memorial Institute medium (RPMI 1640), L-glutamine, nonessential amino acids, penicillin (100 IU mL^{-1}) and streptomycin (100 mg mL^{-1}), ethylenediamine tetraacetic acid (EDTA) and trypsin−EDTA were purchased from HyClone (USA). Human colon carcinoma (Caco-2), lymphocytic Raji B cells and human gastric adenocarcinoma (AGS) cell lines were obtained from American Type Culture Collection (ATCC, USA), and the human colorectal adenocarcinoma modified with methotrexate (HT29-MTX) cells was kindly provided by Dr. T. Lesuffleur (INSERM U178, Villejuif, France).

Preparation of PLGA and PSi Nanoparticles. The nanoparticles composed of PLGA and PSi were prepared as described elsewhere.[7,51,52] The procedure can be found in detail in the SI. Briefly, PLGA nanoparticles were prepared through modified solvent emulsification−evaporation method, based on the water-in-oil-in-water (w/o/w) double emulsion technique using an aqueous solution of PVA 2% as a surfactant. For the PSi nanoparticles, an electrochemical anodization method was used followed by surface modification using undecylenic acid to produce undecylenic modified thermally hydrocarbonized PSi nanoparticles. Both the nanoparticle types, PLGA and PSi, were coated with CS in a ratio of 2:1 (w/w) (CS:nanoparticles) through physical adsorption overnight at room temperature, to form PLGA+CS and PSi+CS nanoparticles, respectively.[7]

CPP Conjugation to the CS-Coated Nanoparticles. The covalent conjugation between the free amine groups in the CS structure with the carboxylic group of CPP was made through the EDC/NHS coupling chemistry. For chemical conjugation, 1 mg of PLGA+CS nanoparticles and 300 μg of PSi+CS were separately dispersed in 1 mL of 10 mM MES containing EDC (final concentration 10 mM) and NHS (final concentration 17 mM) at pH 5.5. CPP was added to this dispersion in a ratio of 1:10 (CPP: nanoparticles) and the nanoparticles were allowed to conjugate overnight in the dark, stirring at 300 rpm originating PLGA+CS-CPP and PSi+CS-CPP, respectively. Afterward, the nanoparticles were collected by centrifugation at 34300*g* for 20 min for PLGA+CS-CPP nanoparticles and at 27600*g* for 5 min for PSi+CS-CPP, and then washed three times with Milli-Q-water.

Enteric Coating of Nanoparticles Using Microfluidics. The GLP-1 loaded nanoparticles were encapsulated into a pH-sensitive polymer (HPMC-AS) using a double emulsion technique, through a microfluidic flow-focusing glass device (Scheme 1),[11] described in detail in the SI. The device consisted of two types of glass capillaries with different diameters, in which the outer diameter of the inner cylindrical tapered capillary fitted the inner dimensions of the outer capillary, facilitating the alignment of their axes.

To prepare the codrug loaded multifunctional systems, 0.5 mg of DPP4 inhibitor was added into 1 mL of 4% of HPMC-AS dissolved in ethyl acetate (oil phase). To this solution, 100 μL of Milli-Q-water containing 20 mg of PLGA+CS-CPP or 200 μg of PSi+CS-CPP (water phase) were added dropwise and homogenized for 30 s using a Vibra-Cell ultrasonic processor (Sonics, Sonics and Matrials, Inc., USA), originating to the first emulsion (w/o). This solution was then poured into a syringe to be injected in the microfluidic device as the inner fluid (oil phase). The outer fluid used was an aqueous solution of 2% Pluronic F127 (water phase). The inner and outer fluids were both pumped into the microfluidic device in opposite directions at 10 and 230 mL h^{-1}, respectively. This flow-focusing geometry forces the inner fluid to breakdown, forming the second monodisperse emulsion (w/o/w) droplets at the entrance orifice of the tapered cylindrical glass capillary. The droplets were collected in a cylindrical beaker containing 80 mL of an aqueous sucrose solution (100 mOsm L^{-1}) in order to facilitate the particles deposition. These particles were solidified through the diffusion of ethyl acetate to the external aqueous phase. As a result, multifunctional systems containing both GLP-1 loaded CS-CPP modified PLGA and PSi nanoparticles and DPP4 inhibitor into a pH-sensitive polymer were obtained, to form the H-PLGA+CS-CPP and H-PSi+CS-CPP respectively.

Particle Characterization. The nanoparticles average size (*Z*-average), PdI and surface charge were analyzed by dynamic light scattering using a Malvern Zetasizer Nano ZS instrument (Malvern Instruments Ltd., UK).

The AE and LD of GLP-1 in the developed nanoparticles were calculated by the difference between the total amount of GLP-1 used to prepare the loaded nanoparticles and the amount of GLP-1 that remained in the aqueous phase, after the nanoparticles isolation by centrifugation, as described elsewhere.[7] The amount of GLP-1 was determined by high performance liquid chromatography (HPLC) (Agilent 1260, Agilent Technologies, USA), using a C_{18} column (4.6 × 150 mm, 5 μm, Supelco Discovery C18, USA). The mobile phase consisted of 0.1% trifluoroacetic acid (pH 2.0) and acetonitrile initially set at the ratio of 70:30 (v/v), which linearly changed to 60:40 (v/v) as a gradient over 5 min. Afterward, the ratio was kept constant for 5 more min. The flow rate was 1.0 mL min^{-1} and the injected volume of the sample was 75 μL. The column temperature was set at room temperature and the detection wavelength at 240 nm. The total area under the curve was used to quantify the GLP-1.

The morphology and surface topography, shape and size of the enteric encapsulated particles were assessed by SEM (SEM, Zeiss DSM 962, Germany).

pH-Sensitive Response of the Multifunctional Particulate Systems. After collection and washing of the particles, they were placed on the SEM supports with double sided carbon adhesive tape. The excess of water was removed with filter paper and different buffer solutions at pH values of 1.2, 4, 5.5, 6.0 and 6.8, were added on top of the particles for 2 h. For pH of 6.0 and 6.8, the 10 min time point was also analyzed. After these time points, the excess of buffer solutions were removed with filter paper and the particles were allowed to dry at room temperature overnight. Afterward, the particles were sputter coated with platinum before visualizing under the SEM.

***In Vitro* Release Studies.** The multifunctional system particles, corresponding to 50 μg of GLP-1, were added separately to 14 mL of pH 1.2 buffer (50 mM KCl) to simulate the gastric fluid and to FaSSIF pH 6.8 (50 mM KH_2PO_4, 15 mM NaOH, 1.0% (w/v) pancreatin) to simulate the fasted state fluid of the intestinal milieu. At specific time points, aliquots of 750 μL were collected and the withdrawn volume was replaced with fresh medium, keeping the volume constant. All the collected aliquots were centrifuged at 27600*g* and the supernatant was used for HPLC analysis in order to quantify the GLP-1 and DPP4 inhibitor released from the systems over time. All the tests were performed at 37 °C and at 100 rpm under sink conditions.

GLP-1 was quantified by HPLC as described above. DPP4 inhibitor was quantified by the total area under the curve through HPLC (Agilent 1260, Agilent Technologies, USA), using a Kinetex 2.6u XB-C18 100A column (4.6 × 75 mm, Phenomenex, USA). The mobile phase consisted of 0.025% of ammonium hydroxide (pH 9.5 adjusted with 50% of phosphoric acid) and acetonitrile set at the ratio of 82:18 (v/v) for 5.5 min. The flow rate was 1.0 mL min^{-1} and the injected volume of the sample was 5 μL. The column temperature was set at room temperature and the detection wavelength at 275 nm.

Cell Culturing. AGS (passage numbers of 10−15) grew in a complete medium consisting of RPMI 1640 supplemented with 10% (v/v) FBS, 1% (v/v) L-glutamine, 1% (v/v) NEAA, and 1% (v/v) antibiotic−antimitotic mixture (final concentration of 100 U mL^{-1} Penicillin and 100 U mL^{-1} Streptomycin). Caco-2 (passage numbers of 31−40) and HT29-MTX (passage numbers of 20−50) cells grew separately in culture flasks in a complete medium consisting of DMEM supplemented in the same way as described before for RPMI. The cells were subcultured once a week using 0.25% trypsin−EDTA to detach the cells from the flasks and seeded at a density of 0.5 × 10^6 cells per 75 cm^2 flask. The culture medium was replaced every other day. Cells were maintained in an incubator (BB 16 gas incubator, Heraeus Instruments GmbH, Germany) at 37 °C and 5- % CO_2 and 95% relative humidity. Raji B cells (passage numbers of 26−35) were cultured in flasks with supplemented DMEM and with the same conditions as described above.

Cell Viability Studies. The viability tests were conducted using the AGS, Caco-2 and HT29-MTX cell lines. Typically, 100 μL of 0.5 × 10^6 cells mL^{-1} were seeded separately in 96-well plates and were allowed to attach overnight. Afterward, the medium was aspirated and the wells were washed twice with 100 μL of prewarmed HBSS−HEPES buffer (pH 7.4). After washing, 100 μL of the nanoparticle solutions at concentrations of 0.1, 0.25, 0.5, and 1 mg mL^{-1} were added to each well, and the plates were incubated at 37 °C for a period of 3 h for AGS, and for 12 h for Caco-2 and HT29-MTX cells. Afterward, the plates were equilibrated at room temperature for about 30 min and then washed twice with 100 μL of fresh HBSS−HEPES buffer (pH 7.4) at room temperature. 50 μL of the reagent assay CellTiter-Glo (Promega Corporation, USA) were added to 50 μL of HBSS−HEPES (pH 7.4) in each well. Negative (HBSS−HEPES buffer, pH 7.4) and positive (1% Triton X-100) control wells were also used and treated similarly as described above. The solutions were mixed and protected from the light for approximately 10 min on an orbital shaker at room temperature. Finally, the luminescence was measured using a Varioskan Flash plate reader (Thermo Fisher Scientific Inc., USA). All data sets were compared with a negative control, considered as 100% viability.

Cell−Nanoparticle Interactions. *Confocal Microscopy Studies.* The intestinal cell−nanoparticle interactions were evaluated through confocal microscopy using a Leica SP5 confocal microscope (Leica Microsystems, Germany). Caco-2 and HT29-MTX were cocultured in a 90:10 ratio (Caco-2/HT29-MTX), in Lab-Tek 8-chamber slides (Thermo Fisher Scientific Inc., USA) and allowed to attach overnight.[7] Then, the cells were washed twice with prewarmed fresh HBSS−HEPES buffer (pH 7.4). 50 μL of Alexa Fluor 488 labeled nanoparticles (see SI) at a concentration of 200 μg mL^{-1} were added to the cells and incubated at 37 °C for 3 h. After incubation, the cells were washed twice with prewarmed fresh HBSS−HEPES buffer (pH 7.4). Afterward, the plasma membrane was stained by adding 200 μL of CellMask Orange (Invitrogen, USA) and incubated for 3 min at 37 °C. The excess of staining solution was washed twice with prewarmed fresh HBSS−HEPES buffer (pH 7.4) and the cells were fixed using 2.5% glutaraldehyde for 20 min.

Flow Cytometry Studies. The quantification of the nanoparticles that are associated with the cells was evaluated using flow cytometry. 1 mL of nanoparticles at a concentration of 300 μg mL^{-1} were added to 0.7 × 10^6 Caco-2/HT29-MTX coculture cells, in a ratio 90:10, in prewarmed HBSS−HEPES buffer (pH 7.4) and incubated at 37 °C for 3 h. Afterward, cells were washed three times with HBSS−HEPES buffer (pH 7.4) and detached with Versene for the measurements. Then, the cells were resuspended in basic sorting buffer that consisted of 1× PBS (Ca/Mg^{2+} free) with 5 mM of EDTA, 25 mM of HEPES and 2% of FBS, to avoid cells aggregation, and analyzed right after using a Beckman Coulter Galios Flow Cytometer with a laser excitation wavelength of 488 nm. The results were analyzed using the software Kaluza Analysis Version 1.3.

Permeability Experiments. For the permeability experiments a triple coculture cell model was used. For that, 7 × 10^4 cells cm^{-3} of Caco-2 and HT29-MTX cells in a ratio of 90:10 were seeded in 12-Transwell cell culture inserts and were allowed to grow and differentiate for 14 days with medium replacement every other day. Then, 1.0 × 10^5 Raji B cell were added to the basolateral chamber for 7 days more in order to induce the phenotype change of Caco-2 cells into M cells and to obtain a triple coculture model.[27] The permeability experiments across the cell monolayers were performed in the apical-to-basolateral direction in HBSS−HEPES (pH 7.4) at 37 °C using an orbital shaker (100 rpm). After removing the cell culture medium, the Transwells were washed twice with prewarmed fresh HBSS−HEPES (pH 7.4) buffer and equilibrated for 30 min. Then, 0.5 mL of nanoparticles corresponding to an amount of 6 μg mL^{-1} of GLP-1 and 40 μg mL^{-1} of DPP4 inhibitor were pipetted into the apical side of the insets. At different time points (15, 30, 60, 120, and 180 min), 100 μL of samples were taken from the basolateral side of the insets and the same volume of prewarmed fresh HBSS−HEPES (pH 7.4) buffer was added to replace the withdrawn volume. Sample concentrations were quantified for GLP-1 by EIA GLP-1 Kit (Sigma-Aldrich, USA) according to manufacturer's instructions and for DPP4 inhibitor by HPLC, as previously described. The integrity of the cell monolayers was checked before and after the permeability experiments by measuring the transepithelial electric resistance using Millicell-Electrical Resistance System (Millipore, USA).

DPP4 Enzymatic Activity. The enzymatic activity of the DPP4 was measured according to the manufacturer's instructions using a DPP4 Activity Assay Kit (Sigma-Aldrich, USA). After the permeability experiments, the cells were washed once with prewarmed HBSS−HEPES buffer (pH 7.4). Then, the cells were lysed with 100 μL of ice-cold Assay Buffer. After lysis, 10 μL of each sample was diluted with Assay Buffer to have a final volume of 50 μL. To each test samples 10 μL of the Assay Buffer was added. To the blank samples, 10 μL aliquots of DPP4 inhibitor were added, mixed well and incubated for 10 min at 37 °C. Afterward, 40 μL of the Master Reaction Mix was added to each test sample and properly mixed and protected from the light. The samples were then incubated for 5 min at 37 °C before starting the fluorescent measurements (λ_{ex} = 360 and λ_{em} = 460). The plate was kept at 37 °C and protected from the light, and the measurements were taken every 5 min for 1 h using a Varioskan Flash plate reader (Thermo Fisher Scientific Inc., USA).

Statistical Analysis. All the experiments were performed in triplicate and represented as mean ± standard deviation. A Student *t*-test and one-way analysis of variance (ANOVA) with Unpaired and Bonferroni post-test (GraphPadPrism, GraphPad software Inc., CA, USA) were used to analyze the data, respectively. The level of significance was set at probabilities of $^*p < 0.05$, $^{**}p < 0.01$, and $^{***}p < 0.001$.

Conflict of Interest: The authors declare no competing financial interest.

Acknowledgment. This work was financed by the European Regional Development Fund (ERDF) through the Programa Operacional Factores de Competitividade − COMPETE, by Portuguese funds through Fundação para a Ciência e a Tecnologia (FCT) in the framework of the project PEst-C/SAU/LA0002/2013, and cofinanced by the North Portugal Regional Operational Programme (ON.2 − O Novo Norte) in the framework of project SAESCTN-PIIC&DT/2011, under the National Strategic Reference Framework (NSRF). Francisca Araújo would like to thank to FCT for financial support (SFRH/BD/87016/2012). Dr. Hélder A. Santos acknowledges financial support from the Academy of Finland (decision no. 252215 and 281300), the University of Helsinki Research Funds, the Biocetrum Helsinki, the Finnish Center for International Mobility (grant no. TM-13-9048), and the European Research Council under the European Union's Seventh Framework Programme (FP/2007−2013, grant no. 310892).

Supporting Information Available: The Supporting Information is available free of charge on the ACS Publications website at DOI: 10.1021/acsnano.5b02762.

Different preparation techniques of the PLGA and PSi nanoparticles, fabrication of a glass-capillary microfluidic flow-focusing device and Alexa Fluor 488 conjugation to nanoparticles. Permeability profiles of GLP-1 from H-PLGA+CS-CPP and H-PSi+CS-CPP particles in the presence and absence of DPP4 inhibitor in a cellular triple coculture model comprised of Caco-2, HT29-MTX and Raji B cells. (PDF)

Note Added after ASAP Publication: This paper was published ASAP on August 5, 2015. The *In Vitro* Cell Viability Studies in the Materials and Methods section was removed due to redundancy and the revised version was reposted on August 10, 2015.

REFERENCES AND NOTES

1. Patel, A.; Patel, M.; Yang, X.; Mitra, A. K. Recent Advances in Protein and Peptide Drug Delivery: A Special Emphasis on Polymeric Nanoparticles. *Protein Pept. Lett.* **2014**, *21*, 1102–1120.
2. Gupta, S.; Jain, A.; Chakraborty, M.; Sahni, J. K.; Ali, J.; Dang, S. Oral Delivery of Therapeutic Proteins and Peptides: A Review on Recent Developments. *Drug Delivery* **2013**, *20*, 237–246.
3. Morishita, M.; Peppas, N. A. Is the Oral Route Possible for Peptide and Protein Drug Delivery? *Drug Discovery Today* **2006**, *11*, 905–910.
4. Araújo, F.; Shrestha, N.; Granja, P. L.; Hirvonen, J.; Santos, H. A.; Sarmento, B. Safety and Toxicity Concerns of Orally Delivered Nanoparticles as Drug Carriers. *Expert Opin. Drug Metab. Toxicol.* **2014**, *11*, 381–393.
5. Gundogdu, E.; Yurdasiper, A. Drug Transport Mechanism of Oral Antidiabetic Nanomedicines. *Int. J. Endocrinol. Metab.* **2014**, *12*, e8984.
6. Santos, H. A.; Mäkilä, E.; Airaksinen, A. J.; Bimbo, L. M.; Hirvonen, J. Porous Silicon Nanoparticles for Nanomedicine: Preparation and Biomedical Applications. *Nanomedicine (London, U. K.)* **2014**, *9*, 535–554.
7. Araújo, F.; Shrestha, N.; Shahbazi, M. A.; Fonte, P.; Mäkilä, E. M.; Salonen, J. J.; Hirvonen, J. T.; Granja, P. L.; Santos, H. A.; Sarmento, B. The Impact of Nanoparticles on the Mucosal Translocation and Transport of GLP-1 across the Intestinal Epithelium. *Biomaterials* **2014**, *35*, 9199–9207.
8. Wang, M.; Zhang, Y.; Feng, J.; Gu, T.; Dong, Q.; Yang, X.; Sun, Y.; Wu, Y.; Chen, Y.; Kong, W. Preparation, Characterization, and *In Vitro* and *In Vivo* Investigation of Chitosan-Coated Poly (D,L-Lactide-Co-Glycolide) Nanoparticles for Intestinal Delivery of Exendin-4. *Int. J. Nanomed.* **2013**, *8*, 1141–1154.
9. Danhier, F.; Ansorena, E.; Silva, J. M.; Coco, R.; Le Breton, A.; Preat, V. Plga-Based Nanoparticles: An Overview of Biomedical Applications. *J. Controlled Release* **2012**, *161*, 505–522.
10. Liu, D.; Bimbo, L. M.; Mäkilä, E.; Villanova, F.; Kaasalainen, M.; Herranz-Blanco, B.; Caramella, C. M.; Lehto, V.-P.; Salonen, J.; Herzig, K.-H.; *et al.* Co-Delivery of a Hydrophobic Small Molecule and a Hydrophilic Peptide by Porous Silicon Nanoparticles. *J. Controlled Release* **2013**, *170*, 268–278.
11. Liu, D.; Zhang, H.; Herranz-Blanco, B.; Mäkilä, E.; Lehto, V. P.; Salonen, J.; Hirvonen, J.; Santos, H. A. Microfluidic Assembly of Monodisperse Multistage pH-Responsive Polymer/Porous Silicon Composites for Precisely Controlled Multi-Drug Delivery. *Small* **2014**, *10*, 2029–2038.
12. Shahbazi, M. A.; Herranz, B.; Santos, H. A. Nanostructured Porous Si-Based Nanoparticles for Targeted Drug Delivery. *Biomatter.* **2012**, *2*, 296–312.
13. Guo, C.; Gemeinhart, R. A. Understanding the Adsorption Mechanism of Chitosan onto Poly(Lactide-Co-Glycolide) Particles. *Eur. J. Pharm. Biopharm.* **2008**, *70*, 597–604.
14. Pereira, C.; Araújo, F.; Granja, P. L.; Santos, H. A.; Sarmento, B. Targeting Membrane Transporters and Receptors as a Mean to Optimize Orally Delivered Biotechnological Based Drugs through Nanoparticle Delivery Systems. *Curr. Pharm. Biotechnol.* **2014**, *15*, 650–658.
15. Sosnik, A.; das Neves, J.; Sarmento, B. Mucoadhesive Polymers in the Design of Nano-Drug Delivery Systems for Administration by Non-Parenteral Routes: A Review. *Prog. Polym. Sci.* **2014**, *39*, 2030–2075.
16. Pedro, A. S.; Albuquerque, A. C.; Ferreira, D.; Sarmento, B. Chitosan: An Option for Development of Essential Oil Delivery Systems for Oral Cavity Care? *Carbohydr. Polym.* **2009**, *76*, 501–508.
17. Sarmento, B.; das Neves, J. *Chitosan-Based Systems for Biopharmaceuticals: Delivery, Targeting and Polymer Therapeutics*. John Wiley & Sons: Hoboken, NJ, 2012.
18. Shi, N. Q.; Qi, X. R.; Xiang, B.; Zhang, Y. A Survey on "Trojan Horse" Peptides: Opportunities, Issues and Controlled Entry to "Troy". *J. Controlled Release* **2014**, *194*, 53–70.
19. Palm-Apergi, C.; Lorents, A.; Padari, K.; Pooga, M.; Hallbrink, M. The Membrane Repair Response Masks Membrane Disturbances Caused by Cell-Penetrating Peptide Uptake. *FASEB J.* **2009**, *23*, 214–223.
20. Wang, F.; Wang, Y.; Zhang, X.; Zhang, W.; Guo, S.; Jin, F. Recent Progress of Cell-Penetrating Peptides as New Carriers for Intracellular Cargo Delivery. *J. Controlled Release* **2014**, *174*, 126–136.
21. Zhang, H.; Liu, D.; Shahbazi, M. A.; Mäkilä, E.; Herranz-Blanco, B.; Salonen, J.; Hirvonen, J.; Santos, H. A. Fabrication of a Multifunctional Nano-in-Micro Drug Delivery Platform by Microfluidic Templated Encapsulation of Porous Silicon in Polymer Matrix. *Adv. Mater.* **2014**, *26*, 4497–4503.
22. Pawar, V. K.; Meher, J. G.; Singh, Y.; Chaurasia, M.; Surendar Reddy, B.; Chourasia, M. K. Targeting of Gastrointestinal Tract for Amended Delivery of Protein/Peptide Therapeutics: Strategies and Industrial Perspectives. *J. Controlled Release* **2014**, *196*, 168–183.
23. Wang, J.; Yadav, V.; Smart, A. L.; Tajiri, S.; Basit, A. W. Toward Oral Delivery of Biopharmaceuticals: An Assessment of the Gastrointestinal Stability of 17 Peptide Drugs. *Mol. Pharmaceutics* **2015**, *12*, 966–973.
24. Janardhan, S.; Sastry, G. N. Dipeptidyl Peptidase Iv Inhibitors: A New Paradigm in Type 2 Diabetes Treatment. *Curr. Drug Targets* **2014**, *15*, 600–621.
25. Duncanson, W. J.; Lin, T.; Abate, A. R.; Seiffert, S.; Shah, R. K.; Weitz, D. A. Microfluidic Synthesis of Advanced Microparticles for Encapsulation and Controlled Release. *Lab Chip* **2012**, *12*, 2135–2145.
26. Liu, D.; Herranz-Blanco, B.; Mäkilä, E.; Arriaga, L. R.; Mirza, S.; Weitz, D. A.; Sandler, N.; Salonen, J.; Hirvonen, J.; Santos, H. A. Microfluidic Templated Mesoporous Silicon-Solid Lipid Microcomposites for Sustained Drug Delivery. *ACS Appl. Mater. Interfaces* **2013**, *5*, 12127–12134.
27. Araújo, F.; Sarmento, B. Towards the Characterization of an *In Vitro* Triple Co-Culture Intestine Cell Model for Permeability Studies. *Int. J. Pharm.* **2013**, *458*, 128–134.
28. Chronopoulou, L.; Massimi, M.; Giardi, M. F.; Cametti, C.; Devirgiliis, L. C.; Dentini, M.; Palocci, C. Chitosan-Coated Plga Nanoparticles: A Sustained Drug Release Strategy for Cell Cultures. *Colloids Surf., B* **2013**, *103*, 310–317.
29. Liu, X.; Liu, C.; Zhang, W.; Xie, C.; Wei, G.; Lu, W. Oligoarginine-Modified Biodegradable Nanoparticles Improve the Intestinal Absorption of Insulin. *Int. J. Pharm.* **2013**, *448*, 159–167.
30. Bu, X.; Zhu, T.; Ma, Y.; Shen, Q. Co-Administration with Cell Penetrating Peptide Enhances the Oral Bioavailability of Docetaxel-Loaded Nanoparticles. *Drug Dev. Ind. Pharm.* **2015**, *41*, 764–771.
31. Kamei, N.; Morishita, M.; Eda, Y.; Ida, N.; Nishio, R.; Takayama, K. Usefulness of Cell-Penetrating Peptides to Improve Intestinal Insulin Absorption. *J. Controlled Release* **2008**, *132*, 21–25.
32. Chen, Y.; Yuan, L.; Zhou, L.; Zhang, Z. H.; Cao, W.; Wu, Q. Effect of Cell-Penetrating Peptide-Coated Nanostructured Lipid Carriers on the Oral Absorption of Tripterine. *Int. J. Nanomed.* **2012**, *7*, 4581–4591.
33. Morishita, M.; Kamei, N.; Ehara, J.; Isowa, K.; Takayama, K. A Novel Approach Using Functional Peptides for Efficient

Intestinal Absorption of Insulin. *J. Controlled Release* **2007**, *118*, 177–184.
34. Liu, D.; Cito, S.; Zhang, Y.; Wang, C.-F.; Sikanen, T. M.; Santos, H. A. A Versatile and Robust Microfluidic Platform towards High Throughput Synthesis of Homogeneous Nanoparticles with Tunable Properties. *Adv. Mater.* **2015**, *27*, 2298–2304.
35. Valencia, P. M.; Farokhzad, O. C.; Karnik, R.; Langer, R. Microfluidic Technologies for Accelerating the Clinical Translation of Nanoparticles. *Nat. Nanotechnol.* **2012**, *7*, 623–629.
36. Herranz-Blanco, B.; Liu, D.; Mäkilä, E.; Shahbazi, M. A.; Ginestar, E.; Zhang, H.; Aseyev, V.; Balasubramanian, V.; Salonen, J.; Hirvonen, J.; *et al.* On-Chip Self-Assembly of a Smart Hybrid Nanocomposite for Antitumoral Applications. *Adv. Funct. Mater.* **2015**, *25*, 1448–1497.
37. Afshari, M.; Derakhshandeh, K.; Hosseinzadeh, L. Characterisation, Cytotoxicity and Apoptosis Studies of Methotrexate-Loaded PLGA and PLGA-PEG Nanoparticles. *J. Microencapsulation* **2014**, *31*, 239–245.
38. Antunes, F.; Andrade, F.; Araújo, F.; Ferreira, D.; Sarmento, B. Establishment of a Triple Co-Culture *In Vitro* Cell Models to Study Intestinal Absorption of Peptide Drugs. *Eur. J. Pharm. Biopharm.* **2013**, *83*, 427–435.
39. Shrestha, N.; Shahbazi, M.-A.; Araújo, F.; Zhang, H.; Mäkilä, E. M.; Kauppila, J.; Sarmento, B.; Salonen, J. J.; Hirvonen, J. T.; Santos, H. A. Chitosan-Modified Porous Silicon Microparticles for Enhanced Permeability of Insulin across Intestinal Cell Monolayers. *Biomaterials* **2014**, *35*, 7172–7179.
40. Kumari, A.; Yadav, S. K. Cellular Interactions of Therapeutically Delivered Nanoparticles. *Expert Opin. Drug Delivery* **2011**, *8*, 141–151.
41. Verma, A.; Stellacci, F. Effect of Surface Properties on Nanoparticle-Cell Interactions. *Small* **2010**, *6*, 12–21.
42. Kilk, K.; Mahlapuu, R.; Soomets, U.; Langel, U. Analysis of *In Vitro* Toxicity of Five Cell-Penetrating Peptides by Metabolic Profiling. *Toxicology* **2009**, *265*, 87–95.
43. Hoshi, N.; Yano, H.; Hirashima, K.; Kitagawa, H.; Fukuda, Y. Toxicological Studies of Hydroxypropylmethylcellulose Acetate Succinate—Acute Toxicity in Rats and Rabbits, and Subchronic and Chronic Toxicities in Rats. *J. Toxicol. Sci.* **1985**, *10* (Suppl. 2), 147–185.
44. Liu, L.; Yang, J.-P.; Ju, X.-J.; Xie, R.; Yang, L.; Liang, B.; Chu, L.-Y. Microfluidic Preparation of Monodisperse Ethyl Cellulose Hollow Microcapsules with Non-Toxic Solvent. *J. Colloid Interface Sci.* **2009**, *336*, 100–106.
45. Mitani, H.; Takimoto, M.; Kimura, M. Dipeptidyl Peptidase Iv Inhibitor Nvp-Dpp728 Ameliorates Early Insulin Response and Glucose Tolerance in Aged Rats but Not in Aged Fischer 344 Rats Lacking Its Enzyme Activity. *Jpn. J. Pharmacol.* **2002**, *88*, 451–458.
46. Reimer, M. K.; Holst, J. J.; Ahren, B. Long-Term Inhibition of Dipeptidyl Peptidase Iv Improves Glucose Tolerance and Preserves Islet Function in Mice. *Eur. J. Endocrinol.* **2002**, *146*, 717–727.
47. Chen, M. C.; Mi, F. L.; Liao, Z. X.; Hsiao, C. W.; Sonaje, K.; Chung, M. F.; Hsu, L. W.; Sung, H. W. Recent Advances in Chitosan-Based Nanoparticles for Oral Delivery of Macromolecules. *Adv. Drug Delivery Rev.* **2013**, *65*, 865–879.
48. Takasaki, K.; Iwase, M.; Nakajima, T.; Ueno, K.; Nomoto, Y.; Nakanishi, S.; Higo, K. K579, a Slow-Binding Inhibitor of Dipeptidyl Peptidase Iv, Is a Long-Acting Hypoglycemic Agent. *Eur. J. Pharmacol.* **2004**, *486*, 335–342.
49. Ahren, B.; Simonsson, E.; Larsson, H.; Landin-Olsson, M.; Torgeirsson, H.; Jansson, P. A.; Sandqvist, M.; Bavenholm, P.; Efendic, S.; Eriksson, J. W.; *et al.* Inhibition of Dipeptidyl Peptidase Iv Improves Metabolic Control over a 4-Week Study Period in Type 2 Diabetes. *Diabetes Care* **2002**, *25*, 869–875.
50. Villhauer, E. B.; Brinkman, J. A.; Naderi, G. B.; Dunning, B. E.; Mangold, B. L.; Mone, M. D.; Russell, M. E.; Weldon, S. C.; Hughes, T. E. 1-[2-[(5-Cyanopyridin-2-Yl)Amino]Ethylamino]-Acetyl-2-(S)-Pyrrolidinecarbonitrile: A Potent, Selective, and Orally Bioavailable Dipeptidyl Peptidase Iv Inhibitor with Antihyperglycemic Properties. *J. Med. Chem.* **2002**, *45*, 2362–2365.
51. Shahbazi, M.-A.; Hamidi, M.; Mäkilä, E. M.; Zhang, H.; Almeida, P. V.; Kaasalainen, M.; Salonen, J. J.; Hirvonen, J. T.; Santos, H. A. The Mechanisms of Surface Chemistry Effects of Mesoporous Silicon Nanoparticles on Immunotoxicity and Biocompatibility. *Biomaterials* **2013**, *34*, 7776–7789.
52. Shahbazi, M. A.; Shrestha, N.; Mäkilä, E.; Araújo, F.; Correia, A.; Ramos, T.; Sarmento, B.; Salonen, J.; Hirvonen, J.; Santos, H. A. A Prospective Cancer Chemo-Immunotherapy Approach Mediated by Synergistic CD326 Targeted Porous Silicon Nanovectors. *Nano Res.* **2015**, *8*, 1505–1521.